Bidirectional Electron Transfer in Photosystem I: Determination of Two Distances between P_{700}^+ and A_1^- in Spin-Correlated Radical Pairs†

Stefano Santabarbara,‡,§ Ilya Kuprov,|| Wendy V. Fairclough,‡,§ Saul Purton,§ Peter J. Hore,|| Peter Heathcote,*,‡ and Mike C. W. Evans*,§

School of Biological Sciences, Queen Mary, University of London, Mile End Road, London E1 4NS, United Kingdom, Department of Biology, University College London, Gower Street, London WC1E 6BT, United Kingdom, and Department of Chemistry, Physical and Theoretical Chemistry Laboratory, University of Oxford, South Parks Road, Oxford OX1 3QZ, United Kingdom

Received July 21, 2004; Revised Manuscript Received November 17, 2004

ABSTRACT: The spin-correlated radical pair $[P_{700}^+A_1^-]$ gives rise to a characteristic "out-of-phase" electron spin−echo signal. The electron spin−echo envelope modulation (ESEEM) of these signals has been studied in thylakoids prepared from the wild-type strain of *Chlamydomonas reinhardtii* and in two site-directed mutants, in which the methionine residue which acts as the axial ligand to the chlorin electron acceptor A_0 has been substituted with a histidine either on the PsaA (PsaA-M684H) or the PsaB (PsaB-M664H) reaction center subunits. The analysis of the time domain ESEEM provides information about the spin−spin interaction in the $[P_{700}^+A_1^-]$ radical pair, and the values of the dipolar (D) and the exchange (J) interaction can be extracted. From the distance dependence of the dipolar coupling term, the distance between the unpaired electron spin density clouds of the primary donor P_{700}^+ and the phyllosemiquinone A_1^- can be determined. The $[P_{700}^+A_1^-]$ ESEEM spectrum obtained in wild-type thylakoids can be reconstructed using a linear combination of the spectra measured in the PsaA and PsaB A_0 mutants, demonstrating that electron transfer resulting in charge separation is occurring on both the PsaA and PsaB branches. The $[P_{700}^+A_{1B}^-]$ distance in the point dipole approximation in the PsaA-M684H mutant is 24.27 ± 0.02 Å, and the $[P_{700}^+A_{1A}^-]$ distance in the PsaB-M664H mutant is 25.43 ± 0.01 Å. An intermediate value of 25.01 ± 0.02 Å is obtained in the wild-type membranes which exhibit both spin-polarized pairs.

Photosystem I (PS I)[1] is a multisubunit protein complex which catalyzes the oxidation of plastocyanin and the reduction of ferredoxin. This reaction center is a heterodimer of the *psaA* and the *psaB* gene products that act both as the inner antenna, coordinating about 100 chlorophyll *a* and about 30 β-carotene molecules, and as the reaction center, binding most of the electron transfer cofactors. Electron transfer is initiated by light absorption and charge separation at the level of the primary donor, P_{700}, which is a special pair of chlorophylls, and the primary electron acceptor, a chlorin molecule, named A_0. The electrons are then transferred to a tightly bound quinone, A_1, and then to a set of [4Fe-4S] iron−sulfur centers, which operate in sequence, F_X, F_A, and F_B (see ref *1* for recent reviews).

In recent years a high-resolution X-ray structure has been obtained for PS I from the thermophilic cyanobacterium *Synechococcus elongatus*, in which the electron transfer cofactors and the surrounding protein have been clearly identified (*2*). The crystal structure shows a highly symmetrical organization of the electron transfer cofactors, around the axis perpendicular to the membrane plane, as previously observed in the structure of the type II purple bacterial reaction center complexes (e.g., refs *3* and *4*). Despite the symmetry in the organization of the electron transfer chains, a large body of evidence has demonstrated that, in purple bacteria, electron transfer only occurs on one branch of the reaction center. In this case it can be argued that the almost perfect symmetry of the system is broken by the fact that one of the quinone molecules, Q_A, is tightly bound and the other, Q_B, can diffuse in the membrane following double reduction and protonation.

Although some experimental evidence can be interpreted to support a model of PS I unidirectional electron transfer (i.e., refs *5*−*10*), a number of observations suggest that both of the electron transfer chains, coordinated by either the PsaA or PsaB subunits of PS I, are active. Data supporting a bidirectional model have been obtained from a combined approach of site-directed mutagenesis and time-resolved

† This work was supported by grants from the U.K. Biotechnology and Biological Sciences Research Council (BBSRC) (CO0350, CO7809, and B18658), a BBSRC studentship to W.V.F., a European Union TMR programme (Contract FMRX-CT98-0214), and funding from the Scatcherd European Foundation and the Hill Foundation for a studentship to I.K.

* To whom correspondence should be addressed. P.H.: phone, 00-44-20-7882-3019; fax, 00-44-20-8983-5489; e-mail, p.heathcote@qmul.ac.uk. M.C.W.E.: e-mail, mike.evans@ucl.ac.uk.

‡ University of London.

§ University College London.

|| University of Oxford.

[1] Abbreviations: PS I, photosystem I; P_{700}, photosystem I primary donor; A_1, phylloquinone acceptor; F_X, iron−sulfur cluster X; ESE, electron spin−echo; ESEEM, electron spin−echo envelope modulation; OOP-ESEEM, ESEEM of the flash-induced out of phase signal in PS I; ESP, electron spin polarization.

10.1021/bi048445d CCC: $30.25
Published on Web 01/20/2005

optical (*11*, *12*) or electron paramagnetic resonance (EPR) spectroscopy (*13*−*15*). Two characteristic times of electron transfer to the iron−sulfur center F_X of 5−10 and 150−200 ns have been reported in different PS I preparations (*6*−*8*) but have been interpreted either as resulting from perturbation of the system due to the preparation procedure or in terms of a "quasi-equilibrium model" of the electron transfer between A_1 and F_X (*6*−*8*). However, Joliot and co-workers (*11*) have presented evidence suggesting that the electron transfer from A_1 to F_X is biphasic in intact cells of the unicellular algae *Chlorella sorokiniana*, a result confirmed in cells of *Chlamydomonas reinhardtii* (*12*), excluding the possibility that the two rates might originate from preparation procedures. Site-directed mutational studies have shown that the faster rate of forward electron transfer from A_1 is modulated by substitutions in the PsaB phylloquinone binding pocket and the slower by corresponding changes in the PsaA (*12*) binding site. Moreover, the A_1^- semiquinones associated with each branch of the electron transfer can also be characterized by different sets of hyperfine couplings determined by ENDOR and are shown to be photoaccumulated under different conditions (*14*).

At room temperature, the rate of decay of the "out-of-phase" electron spin−echo (ESE) signal from the geminate pair $[P_{700}^+A_1^-]$ originally reported by Thurnauer et al. (*16*, *17*) closely matches the 200 ns rate observed by optical spectroscopy for forward electron transport from A_1 to F_X (*16*−*21*). Site-directed mutagenesis of residues in the phylloquinone binding pocket on the PsaA subunit showed that this rate reflects forward electron transfer from A_1 to F_X on the PsaA polypeptide (*21*, *22*). At 100 K forward electron transfer from A_1 to F_X is impaired in about 40% of PS I centers (*8*), and charge recombination can take place. The lifetime for charge recombination between P_{700}^+ and A_1^-, determined by time-resolved optical spectroscopy, was originally suggested to be about 100−200 μs (*7*, *8*). However, subsequent measurements suggested that if F_X is reduced or removed, then two phases of decay are observed, i.e., one of 150 μs and one an order of magnitude faster at 15 μs (*23*, *24*). At cryogenic temperatures the charge recombination reactions can also be monitored by time-resolved EPR because the long-lived $[P_{700}^+A_1^-]$ radical pair state gives rise to an intense spin-polarized EPR spectrum. The decay of the electron spin−echo signal, which is due to a mixture of charge recombination and loss of spin correlation within the $[P_{700}^+A_1^-]$ pair induced by interaction with the protein environment (spin−lattice relaxation), has been reported in the ∼2−20 μs interval (*13*, *15*). In a recent analysis the decay of the light-induced electron spin polarization signal associated with the radical pair $[P_{700}^+A_1^-]$ at 100 K has also been shown to be biphasic in thylakoid preparations from *C. reinhardtii* and *Synechocystis* sp. PCC 6803 (*13*). One decay rate has been suggested to be associated with the PsaA electron transfer branch and one with the PsaB branch (*13*). This interpretation was further confirmed by site-directed mutations at the level of the primary electron donor A_0 (*15*).

An intense modulation of the out-of-phase ESE is observed in two-pulse ESEEM experiments, which, according to a large body of theoretical studies on correlated coupled radical pair models, is not dominated by hyperfine interactions with nuclei but by the dipolar (*D*) and the exchange (*J*) interaction between the electron spins in the radical pair (*25*−*28*). Due to the relatively large distance between the radicals in photosynthetic reaction centers, the dipolar interaction energy is about 2 orders of magnitude bigger than the exchange interaction energy. Therefore, it is the *D* term that dominates the modulation of the ESEEM spectra. The determination of the value of *D* allows estimation of the distance between the electron spins in the radical pair. This approach has led to the successful determination of the distances within spin-correlated radical pairs in photosynthetic systems such as $[P_{865}^+Q_A^-]$ in the reaction center of *Rhodobacter sphaeroides* (e.g., refs *29* and *30*) or $[P_{680}^+Q_A^-]$ and $[Y_Z^+Q_A^-]$ in the PS II RC of higher plants (*31*, *32*). Notably, the distance between P_{700}^+ and the PsaA branch A_1^- in *S. elongatus* PS I particles (*33*, *34*) and single crystals (*35*) has been determined by the ESEEM technique to be 25.4 ± 0.3 Å, a value which has been shown to closely match the X-ray structural data (*2*).

In this paper we present an analysis of the decay and modulation of the out-of-phase electron spin−echo associated with the radical pair $[P_{700}^+A_1^-]$ in *C. reinhardtii* thylakoids purified from wild type and two symmetrical site-directed mutants, PsaA-M684H and PsaB-M664H, in which the axial ligand to the primary electron acceptor, A_0, is changed from a methionine to a histidine on both reaction center subunits.

The analysis was carried out under conditions in which the iron−sulfur acceptor F_X was either oxidized or reduced. The results indicate that two different ESE signals, characterized by different lifetimes and envelope modulations, can be detected in the wild type but are suppressed selectively by the point mutations, leading to independent observation of each ESE signal in the mutants. We interpret these findings in the frame of the bidirectional electron transfer model for PS I electron transfer and suggest that the signal observed arises from the radical pair $[P_{700}^+A_1^-]$ formed on either the PsaA or the PsaB branch of the PS I reaction center. The distance between the spins in the radical pairs is discussed in terms of the X-ray crystallographic data.

EXPERIMENTAL PROCEDURES

C. reinhardtii was grown heterotrophically, and thylakoids were prepared as in ref *15*. Thylakoids were resuspended at 2 mg/mL Chl in buffer containing 50 mM K-HEPES, pH 8, 10 mM NaCl, 5 mM $MgCl_2$, and 100 mM sorbitol.

EPR samples were reduced in the dark at pH 8 under anaerobic conditions with 11.5 mM sodium dithionite for 30 min prior to freezing in liquid nitrogen and either kept dark or illuminated at 205 K for 5 min (*15*). The dark incubation of thylakoids in the presence of the reductant sodium dithionite (E_m = −500 mV) results in a partial reduction of the Fe-S $F_{A/B}$ clusters but little or no reduction of F_X, which has an estimated redox midpoint potential (E_m) in the −(680−730) mV range (*36*−*38*). In photosystem I samples with P_{700} reduced and the iron−sulfur centers oxidized, illumination at 15 K produces an essentially irreversible electron transfer from P_{700} to $F_{A/B}$. If $F_{A/B}$ are prereduced, an oxidation of P_{700} is seen which is reversible over 2.0−300.0 ms at 15 K. Further reduction of F_X suppresses the light-induced P_{700}^+ signal at 15 K (*36*, *37*). The extent of reduction of the iron−sulfur centers (*36*, *37*), and eventually of the quinone acceptors (i.e., refs *39* and *40*), can be increased by illumination at 205 K. To monitor the reduction state of F_X, the ability of the samples to produce

a P_{700}^+ radical and reduce the iron−sulfur clusters $F_{A/B}$ was analyzed by CW-EPR at 15 K. The samples were continuously illuminated in the cavity, and the light minus dark difference spectra recorded. The light-induced difference spectra arising from the reduction of the iron−sulfur cluster $F_{A/B}$ and the oxidation of P_{700} were seen in the dark-adapted, dithionite-reduced, samples. However, no light-induced difference spectra could be detected following a 5 min preillumination of the sample at 205 K (data not presented). These results indicate that electron transfer from P_{700} to the iron−sulfur centers is no longer observed in preilluminated samples as a consequence of the almost complete reduction of iron−sulfur centers ($F_{A/B/X}$). A small stable radical ($g = 2$) is detected following 205 K preillumination which can be identified as arising from photoaccumulated A_1 (*39*, *40*). The quantitative comparison of the signal with the maximum amount of photooxidable P_{700}^+, determined by freezing a matching sample under continuous illumination, indicates that less than 5% of the A_1 associated with a single electron transfer chain is reduced after 5 min illumination at 205 K.

The time-resolved EPR measurements were therefore run either using dark-adapted samples, in which the F_X is mainly oxidized, or in samples preilluminated for 5 min at 205 K, in which F_X is mainly reduced.

Time-Resolved Electron Paramagnetic Resonance. Pulsed EPR spectra, ESEEM spectra, and kinetics were measured using a Bruker ESP380 X-band spectrometer with a variable Q dielectric resonator (Bruker Model 1052 DLQ-H 8907) fitted with an Oxford Instruments CF935 cryostat cooled with liquid nitrogen. Actinic illumination was supplied by a Nd:YAG laser (Spectra Physics DCR-11) with 10 ns pulse duration. The acquisition is triggered by the laser Q-switch and the frequency of the laser set to 10 Hz to avoid interference from "spin-polarized" metastable states decaying with long time constants (i.e., chlorophyll triplet states).

The echo was generated by a standard two-pulse sequence, with a $\pi/2$ pulse length of 16 ns and a π pulse of 32 ns. The initial delay between the pulses (τ) was 112 ns, and ESEEM was measured with a τ increment of 8 ns. The delay from the laser flash, limited by electronic jitter, was 120 ns. The spin−echo amplitude decay for the light-induced charge-separated state was recorded by measuring the initial intensity of the ESE as a function of the delay between the laser flash and the first pulse of the sequence (*41*).

Because of small imperfections in the phase setting, it is possible that stable radicals building up during the flash experiments can contribute to the out-of-phase ESE. To compensate for this, the dark ESE decay was recorded under identical conditions except with no laser flash before and after the flash experiment and was subsequently subtracted from the experimental data.

Data Analysis. The time decay of the ESE has been fitted with a sum of exponential functions, by means of laboratory-written software, using the Levenberg−Marquardt algorithm previously described in detail (*42*). The fit function does not take into account the finite width of the microwave pulse and the spectrometer dead time, so the first 60 ns of the decay has not been taken into consideration during the fitting procedure.

The ESEEM spectrum of a spin-correlated radical pair can be analytically described in a point dipole approximation according to the theoretical study of Salikhov et al. (*25*). In the weak interelectron coupling case, after orientational averaging, the time domain ESEEM spectrum can be described by the expression:

$$S(\tau) = He^{-\tau/T}\int_0^{2\pi}\int_0^{\pi}\sin(\omega_e\tau)\,\sin\theta\,d\theta\,d\phi \qquad (1)$$

where T is the relaxation time and H is the amplitude of the echo modulation signal and ω_e is defined as

$$\omega_e = 2J - 2D(\cos^2\theta - {}^1/_3) \qquad (2)$$

where D is the dipolar interaction and J is the exchange interaction and θ is the angle between the externally applied magnetic field and the vector connecting the two spins in the radical pair.

The parameters were obtained by a nonlinear least-squares fit of the time domain data to eq 1 with a second-order polynomial baseline correction. The integral in eq 1 can be evaluated and written out in terms of Fresnel functions:

$$S(\tau) = \frac{2\pi^{3/2}He^{-\tau/T}}{\sqrt{D\tau}}\left[\sin\left(\frac{2(D+3J)\tau}{3}\right)\mathrm{FrC}\left(2\sqrt{\frac{D\tau}{\pi}}\right) - \cos\left(\frac{2(D+3J)\tau}{3}\right)\mathrm{FrS}\left(2\sqrt{\frac{D\tau}{\pi}}\right)\right]$$

$$\mathrm{FrC}(z) = \int_0^z\cos\left(\frac{\pi u^2}{2}\right)du$$

$$\mathrm{FrS}(z) = \int_0^z\sin\left(\frac{\pi u^2}{2}\right)du \qquad (3)$$

A fourth-order polynomial interpolated look-up table of Fresnel functions was employed to reduce the computation time. The approximation accuracy of the look-up table is better than 1.5×10^{-6} within the operational interval.

To obtain a frequency domain spectrum from the data without introducing truncation artifacts, the missing experimental points of the echo modulation were reconstructed using the theoretical fit. The extrapolated data were then subjected to sine Fourier transformation. Attempts to obtain a consistent reconstruction using other methods (backward linear prediction, backward polynomial extrapolation with the echo intensity at $\tau = 0$ constrained to be zero) were unsuccessful.

The error bounds for the fit parameters have been estimated by applying the Cramer−Rao lower bounds theorem, as previously described by Fursman and Hore (*43*). The error values are consistent with both Monte Carlo calculations and interexperiment statistics, as evaluated by Student's *t*-distribution.

The distance X between the electron spins in the radical pair can be estimated from the value of the dipolar coupling parameter D which is related to interelectron separation:

$$D = -\frac{3g_e\mu_B\mu_0}{8\pi X^3} = -2786X^{-3}\ \mathrm{mT\ \AA^{-3}} \qquad (4)$$

where g_e is the g-factor of the free electron, μ_B is the Bohr magneton, and μ_0 is the magnetic permeability of vacuum. D is in millitesla and X in angstroms.

It is important to note that the distances and the error bounds reported are obtained in the point dipole approxima-

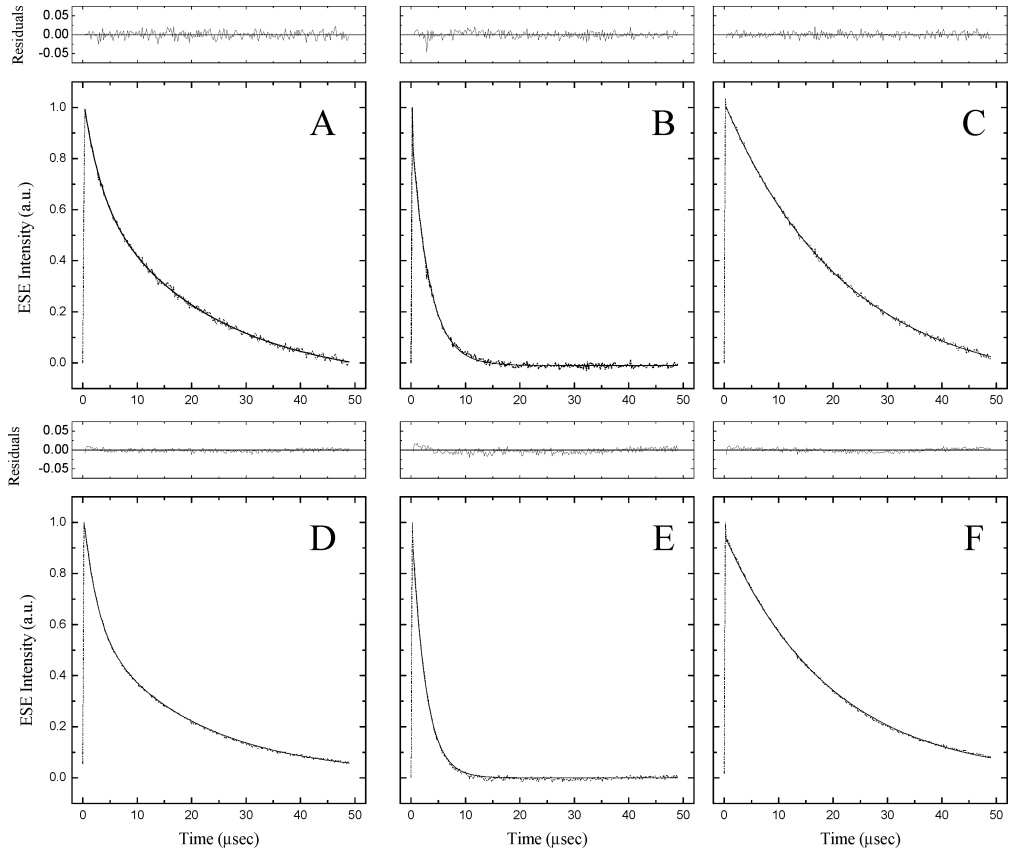

FIGURE 1: Decay of the spin-correlated radical pair $[P_{700}^{+}A_1^{-}]$ in *C. reinhardtii* thylakoids incubated with sodium dithionite at pH 8. Dash-dotted lines are the experimental results; solid lines are the result of the global fitting analysis. The upper panels show the residuals of the fit. (A−C) Wild type, PsaA-M684H, and PsaB-M664H, dark adapted. (D−F) Wild type, PsaA-M684H, and PsaB-M664H, illuminated for 5 min at 205 K. Experimental conditions: field, 346.4 mT; MW frequency, 9.75 GHz; temperature, 100 K.

tion and correspond to the distance between the weighted averages of the spatial distributions of the two unpaired electrons rather than the distance between any particular atoms or groups.

RESULTS

Analysis of the Decay of the Electron Spin−Echo Associated with the Radical Pair $[P_{700}^{+}A_1^{-}]$. Figure 1 presents the decay of the out-of-phase electron spin−echo which originates from the spin-correlated radical pair $[P_{700}^{+}A_1^{-}]$ in thylakoids of wild type and two site-directed mutants, PsaA-M684H and PsaB-M664H, of the green algae *C. reinhardtii* under conditions in which the iron−sulfur cluster F_X is either predominantly oxidized or reduced (see Experimental Procedures for further details). The signals were recorded on the absorptive maximum spin-polarized spectra, which were measured in all of the samples under investigation (data not shown).

The decay of the spin-correlated radical pair in the wild-type thylakoids at 100 K cannot be described by a single exponential, either when the Fe-S clusters are oxidized or when the Fe-S clusters are reduced. The combination of at least two exponential functions, characterized by lifetimes of ∼2 and ∼20 μs, is required to satisfactorily fit the data. On the other hand, the decay can be described by a single exponential in both the PsaA-M684H and the PsaB-M664H mutants, with the first showing only the "fast" ∼2 μs component and the second only the "slow" ∼20 μs component (Figure 1) independent of the redox state of F_X. These values are in close agreement with previous values in wild-type thylakoids from *C. reinhardtii* (*13*, *15*) and *S. elongatus* (*13*). In an attempt to improve the fits, we have applied a global analysis procedure, in which the decays measured in the wild type and the two site-directed mutants, subjected to identical treatments (i.e., oxidized or reduced F_X), are fitted by the same set of lifetimes. The results of this analysis are reported in Table 1. It can be seen that reducing F_X decreases the decay lifetime in all of the samples investigated. This change is small relative to the difference between the two rates and may reflect the effects of the additional spin on the reduced F_X on A_1^{-} spin relaxation. While the decay remains monophasic in both the PsaA-M684H and the PsaB-M664H mutants, it is biphasic in the wild type, and both the lifetimes and the preexponential factors are influenced by the preillumination treatment at low temperature. When the sample is dark adapted (F_X oxidized), the 20 μs component dominates the decay of the ESE in the wild type. This slow phase accounts for almost 80% of the amplitude, leading to an estimate of the average lifetime (τ_{av}) of 16.6 μs. Upon illumination of the thylakoids and reduction of F_X, the total amplitude increases, and the amplitudes of the two phases are almost equally weighted, resulting in an average lifetime of 12.2 μs.

It is also relevant to point out that while the signals presented in Figure 1 are normalized to the maximum in order to better compare the kinetic information, a rather large electron spin−echo can be detected in the dark-adapted membranes from wild type and the PsaB-M664H mutant,

Table 1: Analysis of the Decay of the [$P_{700}^+A_1^-$] Out-of-Phase Electron Spin−Echo[a]

	A_1	τ_1 (μs)	A_2	τ_2 (μs)	τ_{av} (μs)
		Dark-Adapted Thylakoids: Oxidized Iron−Sulfur Center F_X			
wild type	0.24 ± 0.1	3.12 ± 0.03	0.76 ± 0.2	22.22 ± 0.1	17.60 ± 0.2
PsaA-M684H	1	3.12 ± 0.03			3.12 ± 0.3
PsaB-M664H			1	22.22 ± 0.1	22.22 ± 0.1
		205 K Illuminated Thylakoids: Reduced Iron−Sulfur Center F_X			
wild type	0.43 ± 0.2	2.52 ± 0.02	0.57 ± 0.2	19.57 ± 0.2	12.18 ± 0.2
PsaA-M684H	1	2.52 ± 0.02			2.52 ± 0.2
PsaB-M664H			1	19.57 ± 0.2	19.57 ± 0.2

[a] Results of fitting the decay of the electron spin−echo associated with the spin-polarized radical pair [$P_{700}^+A_1^-$] in *C. reinhardtii* thylakoid membrane from the wild type and the PsaA-M684H and the PsaB-M664H mutants. The samples were either dark adapted for 30 min in the presence of the reductant sodium dithionite (pH 8) or preilluminated for 5 min at 205 K. In these conditions the iron-sulfur center F_X is essentially oxidized or reduced. The data have been fitted by a linear sum of exponential functions: $y(t) = \sum_{i=1}^{n} A_i e^{-t/\tau_i}$. The average decay lifetime is defined as $\tau_{av} = \sum_{i=1}^{n} A_i\tau_i / \sum_{i=1}^{n} A_i$.

but the signal observed in the PsaA-M684H mutant is relatively weak. An increase in the signal amplitude is observed in all of the samples after 5 min of illumination at 205 K. In wild type and in the PsaA-M684H dark-adapted samples, illumination at 100 K or below results in oxidation of P_{700} and reduction of $F_{A/B}$, which we would argue is occurring via the PsaB-bound electron transfer branch. Even at 100 K the reversal of this electron transfer is slow relative to the repetition rate used in these experiments. The spin-polarized signal in the reaction centers in which this electron transfer occurs (about half in wild type, nearly all in PsaA-M684H) is not therefore observed in these experiments which depend on repetitive measurements with a repetition time much faster than the decay of the charge separation. Even if conditions were established which allowed repetitive turnover in these reaction centers, the spin-polarized signal would not be resolved as the A_1 to F_X electron transfer on the PsaB branch is thought to have a lifetime of about 20 ns, while the resolution of the spectrometer is limited by laser jitter to ~50 ns. Reduction of F_X prevents forward electron transfer on the PsaB electron transfer branch. Therefore, the lifetime of the [$P_{700}^+A_1^-$] radical pair on this branch is lengthened, and a 2 μs decaying ESP signal can be detected under these conditions.

Analysis of the Out-of-Phase Electron Spin−Echo Envelope Modulation (OOP-ESEEM). As previously mentioned in the introduction and Experimental Procedures sections, modulation of the out-of-phase signal detected in the two-pulse echo experiment is not the result of hyperfine interactions with nuclei but of the dipolar (*D*) and exchange (*J*) interactions between the electrons in the correlated radical pair. Accurate values of the distances between the radical pair partners can be obtained by determining the value of *D*, which is extremely sensitive to changes in interelectron distance, exhibiting an inverse third power dependence (see eq 4 and refs *25*−*35* and *43*).

Figure 2 presents the time dependences of the ESEEM for the wild type and the PsaB-M684H mutant, under conditions where F_X is oxidized. Due to the weakness of the signal in the PsaA-M684H mutant, it was not possible to record a clear envelope modulation of the electron spin−echo under these conditions.

On the other hand, a clear time dependence of the ESEEM is observed in all three samples following 5 min illumination at 205 K (Figure 3). The modulation patterns of the out-of-phase electron spin−echo in the wild type and the PsaA-M684H and the PsaB-M664H strains are significantly different, with the wild type showing an intermediate modulation frequency compared to the two mutants. We have used fittings in the time domain of the ESEEM spectra (*43*), which are shown in Figures 2 and 3 together with the experimental results, to evaluate *D* for each of the preparations. The backward extrapolations of data through the instrument dead time, using the fitted model function, are also shown. Figure 4 shows the sine Fourier transform (SFT) of the data together with the time domain fits, which show excellent agreement. The parameters used to fit the ESEEM spectra are also reported in Table 2.

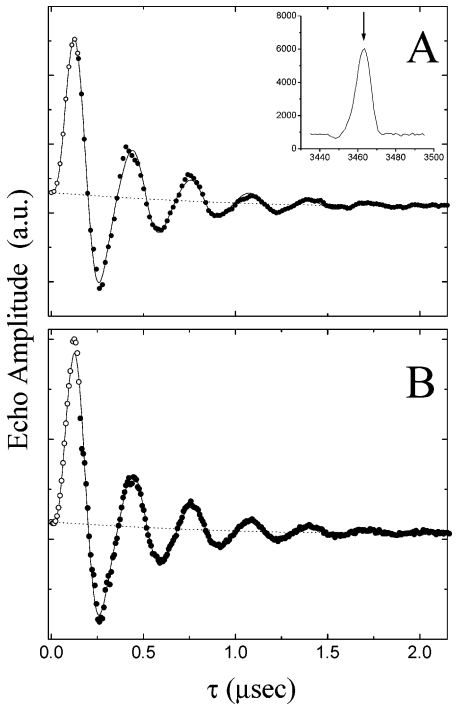

FIGURE 2: Time dependence of the out-of-phase ESEEM associated with the spin-correlated radical pair [$P_{700}^+A_1^-$] in *C. reinhardtii* dark-adapted thylakoids incubated with sodium dithionite at pH 8. Black circles are the experimental results; solid lines are the fit according to eq 3. Open circles are the extrapolation to $\tau = 0$ (see Experimental Procedures for further details). The dashed lines are the second-order baseline correction functions. (A) Wild type; (B) PsaB-M664H. The field-swept ESEEM of the wild-type spectrum is also shown in the insert in panel A; the arrow indicates the field position at which the ESEEM time dependence data are recorded. Experimental conditions as in the caption of Figure 1.

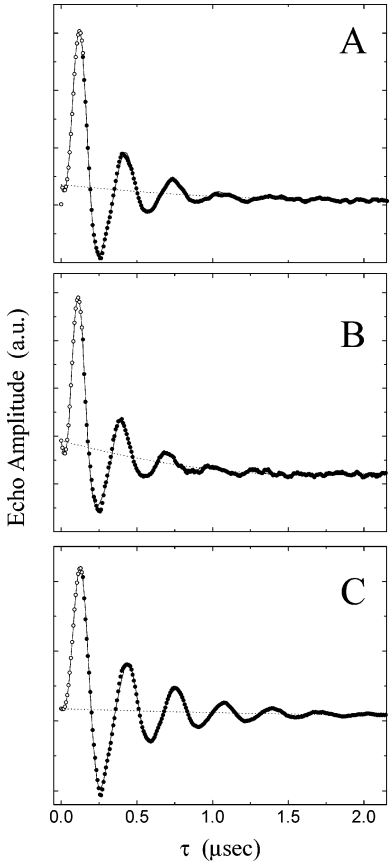

FIGURE 3: Time dependence of the out-of-phase ESEEM associated with the spin-correlated radical pair $[P_{700}^{+}A_1^{-}]$ in *C. reinhardtii* thylakoids preilluminated for 5 min at 205 K. Black circles are the experimental results; solid lines are the fits according to eq 3. Open circles are the extrapolation to $\tau = 0$. The dashed lines are the second-order baseline correction functions. (A) Wild type; (B) PsaA-M684H; (C) PsaB-M664H. Experimental conditions as in the caption of Figure 1.

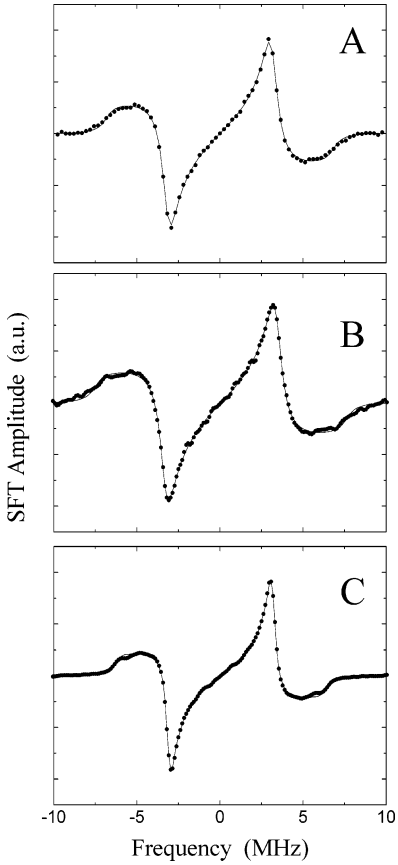

FIGURE 4: Sine Fourier transforms (SFT) of out-of-phase ESEEM signals of the spin-correlated radical pair $[P_{700}^{+}A_1^{-}]$ presented in Figure 3. Black circles are the SFT of the experimental results; solid lines are the SFT of the time domain fit. (A) Wild type; (B) PsaA-M684H; (C) PsaB-M664H.

The fits presented in Figures 2−4 were obtained for unconstrained values of the *D* and the *J* interactions. Since it has been suggested (*25*−*35*) that *J* is vanishingly small because of the distance between the electrons in the radical pairs in photosynthetic systems, we also attempted fitting of the time domain ESEEM signal with *J* constrained to zero. While the results of fitting in the time domain were only slightly worse, this constraint led to a failure in reproducing the frequency domain spectra, especially at the $\nu_{||}$ edge of the SFT (data not shown).

It should be noticed that the theory which describes the time dependence of the out-of-phase ESEEM for a radical pair takes into consideration only the spin−spin interaction within the radical pair. This is expected to be valid for dark-adapted membranes, when the F_X cluster is oxidized and has no net magnetic moment on it. When the F_X cluster is reduced by illumination at low temperature, a third "observer" spin is present, and therefore the model function we use to fit the data can be considered only as an approximation. Some theoretical studies have been published regarding the effect of an observer spin on the EPR spectrum of the radical pair (*44*). However, no evidence has been presented for an effect of a third spin on the "out-of-phase" or "in-phase" ESEEM modulation frequency. Although possible in principle, the effect of additional spin on F_X on the frequency of the ESSEM modulation will be small if F_X^{-} relaxes very

Table 2: Fit Parameters for the Out-of-Phase ESEEM of the Radical Pair $[P_{700}^{+}A_1^{-}]$[a]

	D (μT)	*J* (μT)	*T* (μs)	distance (Å)
Dark-Adapted Thylakoids: Oxidized Iron−Sulfur Center F_X				
wild type	−171.0 ± 0.6	0.6 ± 0.1	0.5868 ± 0.014	25.35 ± 0.03
PsaA-M684H	nd	nd	nd	nd
PsaB-M664H	−169.3 ± 1.7	0.5 ± 0.2	0.6175 ± 0.0067	25.44 ± 0.09
205 K Illuminated Thylakoids: Reduced Iron−Sulfur Center F_X				
wild type	−178.18 ± 0.41	2.21 ± 0.20	0.3879 ± 0.0047	25.01 ± 0.02
PsaA-M684H	−194.84 ± 0.46	4.59 ± 0.22	0.3618 ± 0.0049	24.27 ± 0.02
PsaB-M664H	−171.02 ± 0.29	0.80 ± 0.12	0.6638 ± 0.0075	25.35 ± 0.01

[a] Results of fitting the ESEEM associated with the spin-polarized radical pair $[P_{700}^{+}A_1^{-}]$ in *C. reinhardtii* thylakoid membranes from the wild type and the PsaA-M684H and the PsaB-M664H mutants. The samples were either dark adapted for 30 min in the presence of the reductant sodium dithionite (pH 8) or preilluminated for 5 min at 205 K. In these conditions the iron−sulfur center F_X is essentially oxidized or reduced.

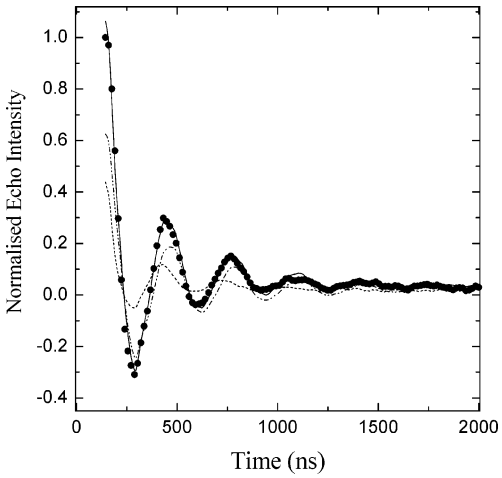

FIGURE 5: Reconstruction of the out-of-phase ESEEM signal of the wild-type *C. reinhardtii* preilluminated thylakoids by a linear combination of the PsaA-M684H and Psa-BM664H ESEEM signals. Open circles, experimental results; solid line, reconstruction of the ESEEM. Scaling factors: 0.41, PsaAM-684H; 0.59, PsaB-M664H. Also shown are the weighted components: dotted line, PsaAM-684H; dash-dotted line, PsaB-M664H.

rapidly compared to the strength of the magnetic interaction between F_X^- and A_1^-, the effective coupling of F_X^- and A_1^- being approximately $(J_{FA})^2T$. Reliable calculations of these exchange interactions are notoriously difficult, and to our knowledge there is no clear estimate of the J_{FA}, while J_{FP} is considered to be zero (*44*−*46*). The spin−lattice relaxation time (T_1) of F_X^- has been estimated at about 1 μs at 8 K (*47*), and it is expected to be much faster at the temperatures at which our ESEEM experiments were performed (100 K). It therefore seems reasonable to assume that this third spin on the reduced F_X cluster will have only a limited effect on the relaxation properties of the $[P_{700}^+A_1^-]$ radical pair.

Furthermore, even if the effective coupling were not small enough to be neglected, this would not mean that the unpaired spin on reduced F_X would necessarily alter the frequency of oscillations in the OOP-ESEEM. In fact, the reduced iron−sulfur center F_X manifests a large *g*-anisotropy, $g_{xx} = 1.76-1.78$, $g_{yy} = 1.86-1.87$, $g_{zz} = 2.06-2.08$ (*36*, *38*), and the EPR spectrum is therefore about 20 mT wide, which is a factor of 20 larger than the bandwidth of the microwave pulses (0.8−1 mT, fwhm) employed in the ESEEM experiments. Hence the magnetic coupling between F_X and A_1 is small for almost all of the reaction center orientations, except the ones in which the EPR frequencies of F_X^- and A_1^- differ less than $(J_{FA})^2T$. Consequently, the presence of a third spin on the reduced F_X centers *only* affects the frequency of oscillations in the OOP-ESEEM when F_X^- (as well as P_{700}^+ and A_1^-) experiences the refocusing pulse. As the EPR spectrum of reduced F_X is strongly anisotropic, it will not be strongly excited by either of the microwave pulses, and no effect on the OOP-ESEEM is therefore expected or observed. Indeed, it should be noticed that the parameters obtained by fitting the data collected from the PsaB-M664H mutant did not differ significantly under conditions where the Fe-S clusters were either oxidized (i.e., no observer spin present) or reduced (Table 2).

From the values of the dipolar coupling parameters *D* obtained from the fitting procedure, distances of 24.27 Å between P_{700}^+ and A_{1B}^- in the PsaA-M684H mutant and 25.35/25.44 Å (F_X oxidized/reduced) between P_{700}^+ and A_{1A} in the PsaB-M664H mutant are obtained. Values of 25.35 and 25.01 Å are obtained for the wild-type membranes when F_X is oxidized or reduced, respectively.

Figure 5 shows the reconstruction of the ESEEM signal recorded in the wild-type thylakoids, in conditions of reduced F_X, using a linear combination of the ESEEM time dependences of the PsaA-M684H and PsaB-M664H mutants, measured under the same conditions. It can be seen that the simulation agrees well with the experimental results and that the weighting factor applied to the normalized spectra is similar to the relative amplitudes derived from the fitting of the echo decay.

DISCUSSION

In wild-type *C. reinhardtii* thylakoids poised at a low redox potential with sodium dithionite, under conditions where the Fe-S cluster F_X is mainly oxidized or entirely reduced, the decay of the electron spin−echo signal due to the radical pair $[P_{700}^+ A_1^-]$ is described by two components having lifetimes of ∼2 and ∼20 μs, the relative amplitudes of which are determined by the reduction state of F_X. In the site-directed mutants of *C. reinhardtii* in which the methionine axial ligand of the chlorin acceptor A_0 has been substituted by a histidine in either the PsaA or the PsaB reaction center subunits, the decay of the electron echo is described by a single exponential function. The reduction of F_X, in both cases, only induced a relatively small change in the decay lifetime, probably due to an increase in magnetic relaxation, as a result of the interaction between the spins on F_X and A_1. It follows that the biphasic decay observed in the wild type is not due to heterogeneity in the reduction state of the Fe-S clusters but rather is due to contributions from both electron transfer branches. These results can be interpreted in terms of the bidirectional model of the electron transfer chain in PS I, suggesting that the lifetime of ∼2 μs is associated with a radical pair formed on the PsaB branch (mutant PsaA-M684H), while the ∼20 μs lifetime is associated with the PsaA branch (PsaB-M664H). The site-directed mutation of the axial ligand to A_0 results in a selective suppression of the ESE signal associated with either the $[P_{700}^+A_{1A}^-]$ or the $[P_{700}^+A_{1B}^-]$ radical pair couples. Ramesh et al. (*48*) have recently observed that identical site-directed mutations, on both reaction center subunits, result in the accumulation of a chlorophyll bleaching, assigned to A_0, on an ∼100 ps time scale. Lengthening the precursor radical pair lifetime ($[P_{700}^+A_0^-]$) can result in increased singlet−triplet mixing. According to the theory of consecutive radical pair states (*45*, *46*, *49*), it can result in the severe quenching or suppression of spin correlation in the subsequent radical pair state, $[P_{700}^+A_1^-]$. From the analysis of the spin-polarized EPR spectrum associated the $[P_{700}^+A_{1A}^-]$ radical pair, Salikhov and co-workers (*50*) have estimated that, in a site-directed mutant in which natural methionine axial ligand to A_0 was substituted with an alanine, the lifetime of the $[P_{700}^+A_{0(A)}^-]$ radical pair was lengthened to about 1 ns, compared to several picoseconds in the wild type. Similar considerations can be extended to the mutants investigated in this study (*45*, *46*, *49*, *50*) and explain the selective suppression of the spin-polarized electron spin−echo on each electron transfer branch.

The ability to independently detect the electron spin-polarized signal arising from each side of the reaction center in the site-directed mutants allows us to measure the ESEEM spectrum of each [$P_{700}^{+}A_1^{-}$] pair. The analysis of the time and frequency domain ESEEM spectra of the PsaA-M664H and PsaB-M684H mutants, in which either one or the other branch of PS I electron transfer is selectively observed, provides information about the exchange (*J*) and the dipolar coupling (*D*) interactions (*25*−*35*, *43*). The determination of the value of *D* is a sensitive tool to estimate the distance between the spins of the spin-correlated radical pair. The fitting of the ESEEM signals results in values of $D_A = -169.3/171.0$ μT, $J_A = 0.5/0.8$ μT (oxidized/reduced, respectively) and $D_B = -194.8$ μT, $J_B = 4.6$ μT which in turn allows calculation of the distance of $X_A = 25.44/25.35$ Å (oxidized/reduced, respectively) between the spin on the primary donor cation P_{700}^{+} and the quinone acceptor A_{1A}^{-} bound to the PsaA subunit and $X_B = 24.27$ Å between P_{700}^{+} and the quinone acceptor A_{1B}^{-} on the PsaB subunit. The spin−spin interaction parameters estimated here for the radical pair formed on the A branch of PS I electron transfer are in close agreement with those determined by Bittl and Zech (*33*) and Dzuba et al. (*34*) in the cyanobacterium *S. elongatus*.

Although it is still about 2 orders of magnitude smaller than the dipolar coupling, a somewhat larger value for the exchange interaction is observed for the PsaB side bound quinone (A_{1B}) compared to values often reported in the literature (*29*−*35*). This is the phyllosemiquinone in which the spin is closer to the primary electron donor cation spin. Therefore, noting that *J* is also sensitive to the spatial distribution of the unpaired electron density, it is not surprising that an increased exchange interaction is detected in this case. Unfortunately, no detailed information about the electron spin distribution in these phyllosemiquinone species is currently available; therefore, the increase in the *J* value can be treated only qualitatively. Intermediate values of $D = -178.2$ μT and $J = 2.2$ μT are found in wild-type membranes, when F_X is reduced, while the parameters are not dissimilar from those found for the PsaB-M664H mutant in the dark-adapted sample (Table 2). Since the ESEEM signal in preilluminated *C. reinhardtii* wild-type membranes can be reasonably well reconstructed by a linear combination of the spectra obtained in the mutants which selectively block electron transfer on either the PsaA or PsaB branches, we suggest that a superposition of two echo envelope modulation profiles originating from radical pairs populated on both reaction center branches is being observed in this case.

Assuming a strong charge delocalization on the PsaB half of the heterodimer constituting the primary donor P_{700}, as suggested by site-directed mutagenesis in combination with proton ENDOR spectroscopy of P_{700}^{+} (*51*−*54*), it is possible to reconcile the distance estimated by ESEEM with the X-ray structure of the PS I core of *S. elongatus* (*2*). A distance of 24.5 Å between the central magnesium of the P_{700B} chlorophyll and the center of the axis connecting the oxygen molecules in the A_{1B} quinone can be estimated from the structure, which is in close agreement with the value of $X_B = 24.27$ Å derived from the time dependence of the ESEEM signals. Similarly, a distance of 26.0 Å is determined between P_{700B} and A_{1A} while a value of $X_A = 25.44$ Å is determined from the ESEEM (see also refs *33*−*35*).

However, there are small discrepancies between the X-ray model and the results obtained by electron spin−echo spectroscopy. It should be emphasized that the distance determined by pulsed EPR relies upon a point dipole approximation and represents a distance between the weighted averages of the electron spin density clouds, which may not correspond to the geometric centers of the cofactors. Moreover, the X-ray structure is determined in a system in which the phylloquinones are in the neutral form, while it is the phyllosemiquinone which is monitored by steady-state and pulsed EPR techniques. A relatively large reorganization energy has been determined for the A_1 to F_X forward electron transport reaction (*7*, *8*, *55*); therefore, the quinone may move within its binding pocket as it is reduced to the phyllosemiquinone. It is clear that if this were the case, the differences between the center-to-center distances estimated from the X-ray structure and the spin−spin distance determined by EPR spectroscopy could easily be reconciled.

ACKNOWLEDGMENT

We thank Drs. S. E. J. Rigby and C. D. Syme (Queen Mary, London) for critical reading of the manuscript and Miss F. O'Boyle for help with analysis of the deposited crystallographic structure.

REFERENCES

1. Heathcote, P., Guest Ed. (2002) *Biochim. Biophys. Acta Bioenergetics Special Issue, Type I photosynthetic reaction centres*, Vol. 1507, pp 1−312, Elsevier, Amsterdam.
2. Jordan, P., Fromme, P., Klukas, O., Witt, H. T., Saenger, W., and Krauss, N. (2001) Three-dimensional structure of cyanobacterial photosystem I at 2.5 angstrom resolution, *Nature 411*, 909−917.
3. Deisenhofer, J., and Michel, H. (1989) The photosynthetic reaction centre from the purple bacterium *Rhodopseudomonas viridis*, *EMBO J. 8*, 2149−2170.
4. El-Kabbani, O., Chang, C.-H., Tiede, D., Norris, J., and Schiffer, M. (1991) Comparison of reaction centers from *Rhodobacter sphaeroides* and *Rhodopseudomonas viridis*: overall architecture and protein−pigment interactions, *Biochemistry 30*, 5361−5369.
5. Biggins, G. S., and Mathis, P. (1988) Functional role of vitamin K1 in photosystem I of the cyanobacterium *Synechocystis* 6803, *Biochemistry 27*, 1494−1500.
6. Setif, P., and Brettel, K. (1993) Forward electron transfer from phylloquinone A1 to iron−sulfur centers in spinach photosystem I, *Biochemistry 32*, 7846−7854.
7. Brettel, K. (1997) Electron transfer and arrangement of the redox cofactors in photosystem I, *Biochim. Biophys. Acta Bioenerg. 1318*, 322−373.
8. Schlodder, E., Falkenberg, M., Gergeleit, M., and Brettel, K. (1998) Temperature dependence of forward and reverse electron transfer from A_1^{-}, the reduced secondary electron acceptor in photosystem I, *Biochemistry 37*, 9466−9476.
9. Yang, F., Shen, G., Schluchter, W. M., Zybailov, B. L., Ganago, A. O., Vassiliev, I. R., Bryant, D. A., and Golbeck, J. H. (1998) Deletion of the PsaF polypeptide modifies the environment of the redox-active phylloquinone (A_1). Evidence for unidirectionality of electron transfer in photosystem I, *J. Phys. Chem. B 102*, 8288−8299.
10. Xu, W., Chitnis, P., Valieva, A., van der Est, A., Brettel, K., Guergova-Kuras, K., Pushkar, J., Zech, S. G., Stehlik, D., Shen, G., Zybailov, B., and Golbeck, J. H. (2003) Electron transfer in cyanobacterial photosystem I: II. Determination of forward electron transfer rates of site-directed mutants in a putative electron transfer pathway from A_0 through A_1 to F_X, *J. Biol. Chem. 278*, 27876−27887.
11. Joliot P., and Joliot, A. (1999) *In vivo* analysis of the electron transfer within photosystem I: Are the two phylloquinones involved?, *Biochemistry 38*, 11130−11136.

12. Guergova-Kuras, M., Boudreaux, A., Joliot, A., Joliot, P., and Redding, K. (2001) Evidence for two active branches for electron transfer in photosystem I, *Proc. Natl. Acad. Sci. U.S.A. 98*, 4437−4442.
13. Muhiuddin, I. P., Heathcote, P., Carter, S., Purton, S., Rigby, S. E. J., and Evans, M. C. W. (2001) Evidence from time-resolved studies of the $P700^{\bullet+}/A_1^{\bullet-}$ radical pair for photosynthetic electron transfer on both the PsaA and PsaB branches of the photosystem I reaction centre, *FEBS Lett. 503*, 56−60.
14. Rigby, S. E. J., Muhiuddin, I. P., Evans, M. C. W., Purton, S., and Heathcote, P. (2002) Photoaccumulation of the PsaB phyllosemiquinone in photosystem I of *Chlamydomonas reinhardtii*, *Biochim. Biophys. Acta Bioenerg. 1556*, 13−20.
15. Fairclough, W. V., Forsyth, A., Evans, M. C. W., Rigby, S. E. J., Purton, S., and Heathcote, P. (2003) Bidirectional electron transfer in photosystem I: electron transfer on the PsaA side is not essential for phototrophic growth in *Chlamydomonas*, *Biochim. Biophys. Acta Bioenerg. 1606*, 43−55.
16. Thurnauer, M. C., Bowman, M. K., and Norris, J. R. (1979) Time-resolved electron spin−echo spectroscopy applied to the study of photosynthesis, *FEBS Lett. 100*, 309−312.
17. Thurnauer, M. C., and Norris, J. R. (1980) An electron spin−echo phase shift observed in photosynthetic algae. Possible evidence for dynamic radical pair interactions, *Chem. Phys. Lett. 284*, 98−102.
18. Moenne-Loccoz, P., Heathcote, P., MacLachlan, D. J., Berry, M. C., Davis, I. H., and Evans, M. C. W. (1994) Path of electron-transfer in photosystem I−direct evidence of forward electron-transfer from A_1 to Fe-S_X, *Biochemistry 33*, 10037−10042.
19. Bock, C. H., van der Est, A. J., Brettel, K., and Stehlik, K. (1989) Nanosecond electron transfer kinetics in photosystem I as obtained from transient EPR at room temperature, *FEBS Lett. 239*, 91−96.
20. van der Est, A. (2003) Light-induced spin polarization in type I photosynthetic reaction centres, *Biochim. Biophys. Acta Bioenerg. 1507*, 212−225.
21. Purton, S., Stevens, D. R., Muhiuddin, I. P., Evans, M. C. W., Carter, S., Rigby, S. E. J., and Heathcote, P. (2001) Site-directed mutagenesis of PsaA residue W693 affects phylloquinone binding and function in the photosystem I reaction center of *Chlamydomonas reinhardtii*, *Biochemistry 40*, 2167−2175.
22. Boudreaux, B., MacMillan, F., Teutloff, C., Algarov, R., Gu, F. F., Grimaldi, S., Bittl, R., Brettel, K., and Redding, K. (2001) Mutations in both sides of the photosystem I reaction center identify the phylloquinone observed by electron paramagnetic resonance spectroscopy, *J. Biol. Chem. 276*, 37299−37306.
23. Brettel, K., and Golbeck, J. H. (1996) Spectral and kinetic characterization of electron acceptor A(1) in a photosystem I core devoid of iron−sulfur centers $F\text{-}_X$, $F\text{-}_B$ and $F\text{-}_A$, *Photosynth. Res. 45*, 183−193.
24. Shinkarev, V. P., Zybailov, B., Vassiliev, I. R., and Golbeck, J. H. (2002) Modelling of the $P700^+$ charge recombination kinetics with phylloquinone and plastoquione-9 in the A_1 site of photosystem I, *Biophys. J. 83*, 2885−2897.
25. Salikhov, K. M., Kandrashkin, Y. E., and Salikhov, A. K. (1992) Peculiarity of the free induction and primary spin−echo signal from spin-correlated radical pairs, *Appl. Magn. Res. 3*, 199−216.
26. Tang, J., Thurnauer, M. C., and Norris, J. R. (1994) Electron spin−echo envelope modulation due to the exchange and dipolar interaction in a spin-correlated radical pair, *Chem. Phys. Lett. 219*, 283−290.
27. Hore, P. J., Hunter, D. A., McKie, C. D., and Hoff, A. J. (1987) Electron paramagnetic resonance of spin-correlated radical pairs in photosynthetic reaction centres, *Chem. Phys. Lett. 137*, 495−500.
28. Kothe, G., Weber, S., Ohmes, E., Thurnauer, M. C., and Norris, J. R. (1994) Transient EPR of light-induced radical pairs: manifestation of zero quantum coherence, *J. Chem. Phys. 98*, 2706−2712.
29. Dzuba, S. A., Gast, P., and Hoff, A. J. (1995) ESEEM study of spin−spin interaction in spin-polarised $P^+Q_A^-$ pair in photosynthetic purple bacterium *Rhodobacter sphaeroides* R26, *Chem. Phys. Lett. 236*, 595−602.
30. Zech, S. G., Bittl, R., Gardiner, A. T., and Lubitz, W. (1997) Transient and pulsed EPR spectroscopy on the radical pair state P_{685}^+ Q_A^- to study light-induced changes in bacterial reaction centres, *Appl. Magn. Res. 13*, 517−529.
31. Zech, S. G., Kurrech, J., Eckert, H.-J., Renger, G., Lubitz, W., and Bittl, R. (1997) Determination of the distance between Y(Z)-ox* and QA-* in photosystem II by pulsed EPR spectroscopy on light-induced radical pairs, *FEBS Lett. 414*, 454−459.
32. Hara, H., Dzuba, S. A., Kawamori, A., Akabori, K., Tomo, T., Satoh, K., Iwaki, M., and Itoh, S. (1997) The distance between P680 and Q_A in photosystem II determined by ESEEM spectroscopy, *Biochim. Biophys. Acta 1322*, 77−87.
33. Bittl, R., and Zech, S. G. (1997) Pulsed EPR study of spin-coupled radical pairs in photosynthetic reaction centres: measurements of the distance between P_{700}^+ and A_1^- in photosystem I and between P_{685}^+ and Q_A^- in bacterial reaction centres, *J. Phys. Chem. B 101*, 1429−1436.
34. Dzuba, S. A., Hara, H., Kawamori, A., Iwaki, M., Itoh, S., and Tsvetkov, Y. D. (1997) Electron spin−echo of spin-polarised radical pairs in intact and quinone-reconstituted plant photosystem I reaction centres, *Chem. Phys. Lett. 264*, 238−244.
35. Bittl, R., Zech, S. G., Fromme, P., Witt, H. T., and Lubitz, W. (1997) Pulsed EPR structure analysis of photosystem I single crystals: localisation of phylloquinone acceptor, *Biochemistry 26*, 12001−12004.
36. Evans, M. C. W., Sihra, C. K., and Cammack, R. (1976) The properties of the primary electron acceptor in the photosystem I reaction centre of spinach chloroplasts and its interaction with P700 and the bound ferredoxin in various oxidation−reduction states, *Biochem. J. 158*, 71−77.
37. Evans, M. C. W. (1982) in *Iron Sulphur Proteins* (Spiro, T. G., Ed.) pp 249−284, John Wiley and Sons, New York.
38. Vassiliev, I. R., Antonkine, M. L., and Goldbeck, J. H. (2001) Iron−sulphur clusters in type I reaction centres, *Biochim. Biophys. Acta 1507*, 139−160.
39. Heathcote, P., Hanley, J. A., and Evans, M. C. W. (1993) Double-reduction of A_1 abolishes the EPR signal attributed to A_1^-—evidence for C2 symmetry in the photosystem I reaction-center, *Biochim. Biophys. Acta 1144*, 54−61.
40. MacMillan, F., Hanley, J. A., van der Weerd, L., Knupling, M., Un, S., and Rutherford, A. W. (1997) Orientation of the phylloquinone electron acceptor anion radical in photosystem I, *Biochemistry 36*, 9297−9303.
41. Evans, M. C. W., Purton, S., Patel, V., Wright, D., Heathcote, P., and Rigby, S. E. J. (1999) Modification of electron transfer from the quinone electron carrier, A_1, of photosystem 1 in a site directed mutant D576⇒L within the Fe-S_X binding site of PsaA and in second site suppressors of the mutation in *Chlamydomonas reinhardtii*, *Photosynth. Res. 61*, 33−42.
42. Santabarbara, S., Bordignon, E., Jennings, R. C., and Carbonera, D. (2002) Chlorophyll triplet states associated with photosystem II of thylakoids, *Biochemistry 41*, 8184−8194.
43. Fursman, C. E., and Hore P. J. (1999) Distance determination in spin-correlated radical pairs in photosynthetic reaction centres by electron spin−echo envelope modulation, *Chem. Phys. Lett. 303*, 593−600.
44. Salikhov, K. M., Zech, S. G., and Stehlik, D. (2002) Light induced radical pair intermediates in photosynthetic reaction centres in contact with an observed spin label: spin dynamics and effect on transient EPR spectra, *Mol. Phys. 100*, 1311−1321.
45. Kandrashkin, Y. E., Salikhov, K. M., van der Est, A., and Stehlik, D. (1998) Electron spin polarisation in consecutive spin-correlated radical pairs: application to the short-lived and long live-precursor in type I photosynthetic reaction centres, *Appl. Magn. Res. 15*, 417−447.
46. Kandrashkin, Y. E., and van der Est, A. (2001) A new approach to determining the geometry of weakly coupled radical pairs from their electron spin polarization patterns, *Spectrochim. Acta 57*, 1697−1707.
47. Berry, M. C., Bratt, P. J., and Evans, M. C. W. (1997) Relaxation properties of the photosystem 1 electron transfer components: indications of the relative positions of the electron transfer cofactors in photosystem 1, *Biochim. Biophys. Acta 1319*, 163−176.
48. Ramesh, V. M., Gibasiewicz, K., Lin, S., Bingham, S., and Webber, A. N. (2004) Bidirectional electron transfer in photosystem I: accumulation of A_0^- in A-side or B-side mutants of the axial ligand to chlorophyll A_0, *Biochemistry 43*, 1369−1375.
49. Kandrashkin, Y. E., Vollmann, W., Stehlick, D., Salikhov, K. M., and van der Est, A. (2002) The magnetic field dependence of the electron spin polarisation in consecutive spin correlated radical pairs in type I photosynthetic reaction centres, *Mol. Phys. 100*, 1431−1443.

50. Salikhov, K. M., Pushkar, Y. N., Golbeck, J. H., and Stehlik, D. (2003) Interpretation of the multifrequency transient EPR spectra of the $P_{700}^{+}A_0Q_K^{-}$ state in photosystem I particles with a sequential correlated radical pair model: wild type versus A_0 mutants, *Appl. Magn. Res. 24*, 467−482.
51. Rigby, S. E. J., Nugent, J. H. A., and O'Malley, P. J. (1994) ENDOR and special triple resonance studies of chlorophyll cation radicals in photosystem 2, *Biochemistry 33*, 10043−10050.
52. Krabben, L., Schlodder, E., Jordan, P., Carbonera, D., Giacometti, G., Lee, H., Webber, A. N., and Lubitz, W. (2000) Influence of the axial ligands on the spectral properties of P700 of photosystem I: A study of site-directed mutants, *Biochemistry 39*, 13012−13025.
53. Kass, H., Fromme, P., Witt, H. T., and Lubitz, W. (2001) Orientation and electronic structure of the primary donor radical cation P_{700}^{+} in photosystem I: A single crystals EPR and ENDOR study, *J. Phys. Chem B 105*, 1225−1239.
54. Petrenko, A., Maniero, A. L., van Tol, J., MacMillan, F., Li, Y., Brunel, L.-C., and Redding, K. (2004) A high-field EPR study of P_{700}^{+} in wild-type and mutant photosystem I from *Chlamydomonas reinhardtii*, *Biochemistry 43*, 1781−1786.
55. Brettel, K., and Leibl, W. (2001) Electron transfer in photosystem I, *Biochim. Biophys. Acta Bioenerg. 1507*, 100−114.

BI048445D